npg

Abnormalities in White Matter Microstructure Associated with Chronic Ketamine Use

R Edward Roberts[1], H Valerie Curran[1], Karl J Friston[2] and Celia JA Morgan*[1,3]

[1]Clinical Psychopharmacology Unit, Research Department of Clinical Psychology, University College London, London, UK; [2]Wellcome Trust Centre for Neuroimaging, University College London, London, UK; [3]Department of Psychology, University of Exeter, Exeter, UK

Ketamine is an N-methyl-D-aspartate (NMDA) receptor antagonist that has been found to induce schizophrenia-type symptoms in humans and is a potent and fast-acting antidepressant. It is also a relatively widespread drug of abuse, particularly in China and the UK. Acute administration has been well characterized, but the effect of extended periods of ketamine use—on brain structure in humans—remains poorly understood. We measured indices of white matter microstructural integrity and connectivity in the brain of 16 ketamine users and 16 poly-drug-using controls, and we used probabilistic tractography to quantify changes in corticosubcortical connectivity associated with ketamine use. We found a reduction in the axial diffusivity profile of white matter in a right hemisphere network of white matter regions in ketamine users compared with controls. Within the ketamine-user group, we found a significant positive association between the connectivity profile between the caudate nucleus and the lateral prefrontal cortex and dissociative experiences. These findings suggest that chronic ketamine use may be associated with widespread disruption of white matter integrity, and white matter pathways between subcortical and prefrontal cortical areas may in part predict individual differences in dissociative experiences due to ketamine use.

Neuropsychopharmacology (2014) **39**, 329–338; doi:10.1038/npp.2013.195; published online 2 October 2013

Keywords: ketamine; addiction; schizophrenia; white matter; connectivity; glutamate

INTRODUCTION

Ketamine is a dissociative anesthetic drug that acts primarily via antagonism of glutamatergic N-methyl-d-aspartate (NMDA) receptors. In the past decade, recreational ketamine use has become widespread, particularly in the UK and China. Acute administration of ketamine in healthy volunteers impairs performance on memory and cognitive tasks and also induces psychotic symptoms such as delusions and dissociative sensations (Krystal *et al*, 1994; Morgan *et al*, 2004a). Neuroimaging studies have reported that acute ketamine administration is associated with task-related reductions in prefrontal cortical activation, as measured by blood oxygenation level-dependent (BOLD) response (Corlett *et al*, 2006; Corlett *et al*, 2007). Frequent ketamine use has been found to be associated with persistent working memory and executive function impairment and psychotic-like symptoms (Morgan *et al*, 2004b, 2010). In a longitudinal study, working-memory-impairment change over a year was highly correlated with change in ketamine use over the same time frame, strongly suggesting that this is a drug-induced effect and not a pre-existing difference (Morgan *et al*, 2010). In order to explore the neurobiological basis for the behavioral changes associated with chronic ketamine, positron emission tomography (PET) has been used to measure D1 dopaminergic receptor availability. Narendran *et al* (2005) found significant upregulation of D1 availability in the dorsolateral prefrontal cortex (DLPFC), consistent with a pattern of dopamine depletion, although the degree of D1 receptor ligand binding in DLPFC was not significantly correlated with performance on an n-back working memory task. The neuroimaging data in humans are broadly consistent with the findings of animal studies where treatment with chronic non-competitive NMDA antagonists is associated with reduced prefrontal dopamine levels and impaired performance on tasks sensitive to prefrontal function such as working memory (Verma and Moghaddam, 1996; Brozoski *et al*, 1979; Jentsch and Roth, 1999). A possible explanation of these data is that the behavioral changes associated with ketamine use may be a result of frontal 'hypofunctionality'—a hypofunctionality that may be underpinned by functional disconnection from subcortical systems or afferent (temporoparietal) cortical areas.

Despite some progress in identifying changes in behavior and brain function following heavy ketamine use, our current understanding of the effects of ketamine on the brain structure is poor. A recent study explored whether chronic ketamine users exhibited changes in brain white matter microstructure using magnetic resonance diffusion tensor imaging (DTI) (Liao *et al*, 2010). This technique uses

*Correspondence: Dr CJA Morgan, Clinical Psychopharmacology Unit, Research Department of Clinical Psychology, University College London, Gower Street, London WC1E 6BT, UK, Tel: +442076791932, Fax: +442075931898, E-mail: c.morgan@ucl.ac.uk

the passive diffusion of water molecules in the brain tissue to infer properties of the underlying microarchitecture (Basser *et al*, 1994). The distribution of water diffusion within a voxel, often given as fractional anisotropy (FA), is thought to reflect properties of the white matter microstructure such as axonal size, density and level of myelination (Beaulieu, 2002). Liao *et al* reported significant reductions in FA in the bilateral frontal cortex and the left temporoparietal cortex in chronic ketamine users compared with controls. Individual variability in the level of FA in the frontal cortex was found to correlate negatively with lifetime ketamine consumption (Liao *et al*, 2010). Another study also reported decreased bilateral frontal gray matter volume in chronic ketamine users (Liao *et al*, 2011).

Although these investigations demonstrate that ketamine may be associated with disturbances of brain structure, we cannot conclude from these regional data whether these changes are caused or associated with alterations in connectivity. Aberrant or dysfunctional connectivity is particularly prescient from the point of view of ketamine models of psychosis and disconnection theories of schizophrenia—particularly, in light of disconnections involving the prefrontal cortex. The aim of our study was to advance these investigations by examining both white matter structural integrity and connectivity profiles between cortical and subcortical brain regions thought to be affected by chronic ketamine use.

We investigated whether chronic ketamine users differ from healthy volunteers in terms of generalized white matter structure and the focal connectivity profile of the caudate nucleus with the prefrontal cortex. The rationale for this was as follows. There is evidence to suggest that individual differences in BOLD activation levels in prefrontal and subcortical brain regions under placebo predict the level of psychotic disturbance after acute administration (Honey *et al*, 2008), and the DLPFC and caudate nucleus show differential activation during acute ketamine use on an associative learning task (Corlett *et al*, 2006). In addition, preclinical studies have found that acute ketamine disrupts prefrontal and thalamic connectivity (Dawson *et al*, 2011). As the caudate nucleus is highly innervated by dopaminergic inputs and is thought to have an important role in learning and memory via connections with prefrontal cortical areas, long-term, heavy use of NMDA antagonists might have a significant effect on the structure of such systems. Indeed, recent evidence suggests disruption to caudal activation on a navigation task in chronic ketamine users (Morgan *et al*, submitted). Thus, we hypothesized that the structural connectivity between the caudate nucleus and the prefrontal cortex might be impaired by chronic ketamine use. We focused our analysis on three subregions of the prefrontal cortex: DLPFC; medial prefrontal cortex (MPFC); and orbitofrontal cortex (OFC). This allowed us to determine whether structural changes associated with drug use were because of generalized impaired connectivity or focal disruption of connections to a specific region within the prefrontal cortex. We employed a voxel-wise analysis of white matter structure to search for differences in white matter and then used probabilistic diffusion tensor tractography to examine whether the distribution of connections between the caudate nucleus and the prefrontal cortex differed between control and ketamine-user groups.

Finally, we tried to establish the predictive validity of any disconnections by testing for significant associations with drug use or dissociative and schizotypal side effects.

MATERIALS AND METHODS

Participant Recruitment

Participants were recruited via our existing subject database. Those participants were selected who were (i) frequent ketamine users (using the drug more than three times a week), or (ii) polydrug users who were matched with the current ketamine-using groups for other drug use. All participants were right-handed. A total of 20 controls were recruited but four were excluded—two had adverse reactions in the scanner, one had a positive urine screen for ketamine, and one had to be excluded because of large movement artefacts; 17 ketamine users were recruited but one was excluded because of inability to continue the scanning due to urinary problems (ketamine-induced cystitis). The study was approved by the institutional ethics committee. All subjects were compensated for participation.

Questionnaires

All participants gave a full drug history and completed the Brief Oxford-Liverpool Inventory of Feelings and Experiences (OLIFE; Mason *et al*, 1995) that indexes psychotic-like symptoms in a healthy population and Dissociative Experiences Scale (DES; Bernstein and Putnam, 1986) that taps dissociative symptomatology. The 'Spot the word' test (Baddeley *et al*, 1993) was used as an index of premorbid IQ. The participants also performed an additional associative learning task while in the scanner, details of which are reported elsewhere (Morgan *et al*, 2010).

MRI Acquisition

T1 acquisition. A 3D structural MR image was acquired from each subject using a T1-weighted MDEFT sequence (176 slices, 1 mm thickness, sagittal, phase encoding in anterior/posterior, (FoV) 224×256 mm^2, matrix 224×256, TR = 20.66 ms, TE = 8.42 ms, TI = 640 ms, flip angle 25°, fat saturation, and bandwidth 178 Hz/Pixel) (Deichmann *et al*, 2004).

Diffusion-weighted image acquisition. Diffusion-weighted imaging data were acquired using a 1.5T Sonata Scanner (Siemens, Erlangen, Germany) at the Wellcome Trust Centre for Neuroimaging, London. An echo planar sequence with a double spin-echo module was used to reduce the effect of eddy currents (Reese *et al*, 2003). Each volume consisted of 60 contiguous axial slices of 2.3 mm thickness, with an acquisition matrix of 96×96 in a field of view of 220×220 mm^2, resulting in 2.3 mm^3 isotropic voxels (inter-slice temporal separation = 160 ms, TE = 90 ms, flip angle 90°, fat saturation, and bandwidth 2005 Hz/pixel). Interleaved slice sampling was chosen to avoid cross-talk between adjacent slices. Each DTI data set consisted of 61 high-diffusion-weighted images ($b = 1000$ s mm^{-2}), with diffusion gradients applied along 61 evenly distributed diffusion directions, obtained from the optimization procedure in the study of Jansons and Alexander (2003),

and seven additional images with minimal diffusion weighing ($b = 100 \, \text{s} \, \text{mm}^{-2}$) also with evenly distributed directions. Data acquisition was cardiac-gated to reduce motion artefacts because of pulsation of the cerebrospinal fluid (Wheeler-Kingshott et al, 2002).

Diffusion-weighted imaging preprocessing. DTI processing was performed using tools from the FMRIB Software Library diffusion toolbox (http://www.fmrib.ox.ac.uk/fsl/). Images were corrected for distortions because of eddy currents, and the FSL Brain Extraction Tool (BET) was used to remove non-brain tissue from the diffusion images (Smith, 2002). The diffusion parameters were estimated and a probability distribution function generated for each voxel in the brain. Probabilistic tractography was conducted by sending 5000 samples through each caudate mask. FA images were also created by fitting a tensor model to the raw diffusion data.

Voxel-wise analysis. Voxel-wise analysis of the diffusion data for each participant was conducted using tract-based spatial statistics (Smith et al, 2006), part of FSL (Smith et al, 2004). All participants' FA data were then aligned into a common space using the nonlinear registration tool FNIRT. A mean FA image was created and thinned to generate a mean FA skeleton that represents the centers of all tracts common to the group. Each participant's aligned FA data were then projected onto this skeleton. Axial (D_P) and radial diffusivity (D_R) maps were then generated using these data. The resulting data were used for between group and within-subject voxelwise statistical analysis.

The diffusion profile within each voxel is comprised of the primary, axial direction of diffusion (D_P, which is usually parallel to the axonal fibbers) and the orthogonal secondary and tertiary components, which can be averaged to give the radial diffusivity (D_R). Although a number of studies have combined the three principal diffusivity measurements into a single value, FA, we chose to investigate the axial and radial components of diffusivity separately. There is evidence to suggest that radial diffusivity may be related to the degree of myelination, whereas the axial diffusivity is thought to be more closely related to the level of axonal density (Song et al, 2003; Song et al, 2005). Therefore, by examining radial and axial components separately, this may provide more detailed information about the structural basis for any differences observed.

A voxel-wise whole-brain comparison analysis (ketamine group vs controls) was performed to compare the levels of D_R and D_P throughout the brain, with age included as a covariate of no interest. Results were considered significant for contiguous clusters of > 20 voxels and significance level of $P < 0.05$, corrected for multiple comparisons using threshold-free cluster enhancement (TFCE). This approach avoids the choice of an arbitrary threshold for initial cluster formation (Nichols and Holmes, 2002). In addition, we performed a secondary comparison analysis between the groups to test for the laterality of our findings by restricting the volume of interest to either the right or the left hemisphere. We also tested for hemisphere by group interactions using the TBSS_sym function in FSL to directly compare adjacent white matter regions in each hemisphere.

This procedure generates a symmetric skeleton by using the original (asymmetric) skeleton and dilating it by one voxel. The symmetric mean FA image is generated by flipping and averaging the mean FA map and then skeletonizing to generate the initial symmetric skeleton. This is masked by the dilated original skeleton to ensure that only those areas that are already close to being symmetric in the original data are included. Finally, the skeleton is flipped and masked with the non-flipped version, creating a symmetrized skeleton, from which a thresholded skeleton mask and derived distance map were generated. The location of the clusters was determined using the atlases developed by the Research Center Jülich histological atlas (Eickhoff et al, 2005), and the ICBM-DTI-81 white matter labels and tractography atlases developed by the Laboratory of Brain Anatomical MRI, Johns Hopkins University atlas (Mori et al, 2005; Wakana et al, 2007).

Probabilistic tractography. We used probabilistic tractography to examine the connectivity profile between the caudate nucleus and three major prefrontal areas: lateral prefrontal cortex (LPFC), medial frontal cortex (MFC), and orbital frontal cortex (OFC). Two standard measures of connectivity were employed. Total percentage connectivity was measured by calculating the number of samples from any voxel in the caudate, reaching a specific region of interest (ROI) normalized by the total number of samples from all voxels in the seed mask reaching any ROI. This measure is an index of the degree of connectivity between the seed region (caudate) and a particular cortical ROI, regardless of the origin of the seed voxel in the seed region. We also calculated the connectivity-defined regions (CDRs) for each seed region. This measure employs a threshold to identify those voxels in which > 25% of samples terminate in a particular ROI. This value is normalized by the total number of voxels in the seed region. This index provides a surrogate-clustering index to distinguish between diffuse connectivity throughout a seed region and the localized areas of connectivity. This approach has previously been shown to reflect histologically defined boundaries in the thalamocortical projections (Behrens et al, 2003).

The Freesurfer software package (http://surfer.nmr.mgh. harvard.edu) was used to independently generate three cortical ROIs in each hemisphere using the T1-weighted images. ROIs were composed of subregions generated using Freesurfer cortical parcellations (Desikan et al, 2006). The following three cortical ROIs were employed here: LPF (pars triangularis, frontal pole, rostral middle frontal gyrus, and pars opercularis), MFC (caudal anterior cingulate, rostral anterior cingulate, and superior frontal gyrus) and OFC (pars orbitalis, medial OFC, and lateral OFC) (see Figure 1). Each individual's parcellated data were inspected to ensure consistent segmentation of cortical regions. To preprocess the ROIs for use in the probabilistic tractography software, we followed an approach recently outlined by Marenco et al (2011). The FSL tool FLIRT was used to generate transformation matrices from diffusion to structural space using a normalized mutual information cost function with 12 degrees of freedom. The inverse of the transformation matrices were then used to transform the binary cortical ROIs into diffusion space for use in the tractography
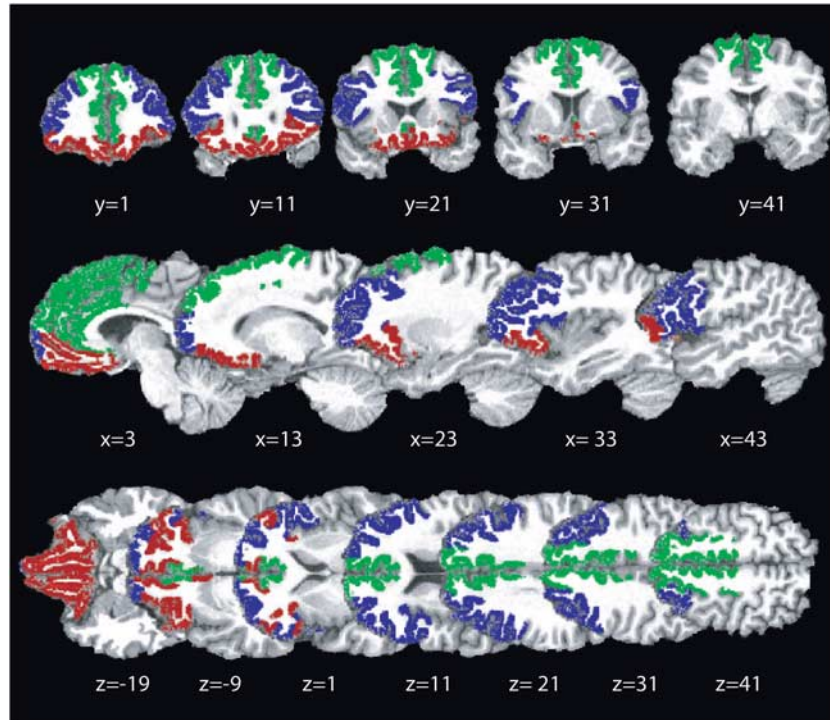
Figure 1 Cortical regions of interest. Cortical regions of interest used in the probabilistic analysis are shown superimposed on a T1-weighted structural image for a representative subject. ROIs were composed of subregions determined using Freesurfer cortical parcellations (Desikan et al, 2006). Three cortical ROIs were employed: lateral prefrontal cortex (blue; pars triangularis, frontal pole, rostral middle frontal gyrus, pars opercularis), medial frontal cortex (green; caudal anterior cingulate, rostral anterior cingulate, superior frontal gyrus), and orbitofrontal cortex (red; pars orbitalis, medial orbitofrontal cortex, lateral orbitofrontal cortex). Locations are given in MNI coordinates.

analysis. Once in diffusion space, the ROIs were thresholded at 0.3, binarized, and corrected to remove overlapping between adjacent regions. Additionally, each ROI was multiplied by the FA image for each subject thresholded at 0.2 to remove any areas of white matter. The caudate ROIs were thresholded at 0.6 and binarized. These thresholds were based on those employed by Marenco et al (2011) and checked against the structural- and diffusion-weighted images (see Figure 1). Data from one participant in the control group were excluded, as the cortical ROIs could not be consistently generated for both hemispheres.

RESULTS

Demographics

There were no significant demographic differences between ketamine ($n = 16$) and control ($n = 16$) groups in terms of age (t (31) = 0.67, $P > 0.50$), gender ($\chi^2 = 0.78$, $P > 0.38$), or years of education (t (31) = 0.93, $P > 0.36$) (Table 1). Ketamine users had significantly greater scores on both the DES (t(31) = 4.64 $P < 0.001$) and OLIFE (t(31) = 3.38, $P < 0.001$). There were no significant group differences in the use of MDMA, alcohol, cannabis, cocaine, or amphetamine or benzodiazepines (See Table 1).

Diffusion Tensor Imaging Results: Voxel-Wise Analysis

Whole-brain comparisons were performed between the ketamine-user and control groups for both axial and radial

diffusivity measures. This comparison analysis 'ketamine < controls' revealed eight clusters of white matter in the right hemisphere of the ketamine group, in which the level of axial diffusivity was significantly lower than that in the control group (see Figure 1 and Table 2). Three clusters were located in the frontal cortex, with the largest one in the region of the anterior corona radiata and inferior fronto-occipital fasciculus (IFOF) (671 voxels). The second cluster lays in the forceps minor (177 voxels), with the third frontal cluster in the anterior forceps minor (34 voxels). There was also a cluster in the white matter of an area, which includes the sagittal stratum, inferior longitudinal fasciculus (IFL), and IFOF (38 voxels). There were two large clusters adjacent to the parietal cortex, the first in the superior longitudinal fasciculus adjacent to the intraparietal sulcus (173 voxels) and the second lying more inferiorly close to the posterior thalamic radiation and the posterior extent of IFOF (165 voxels). The remaining two clusters were located close to the SLF and primary somatosensory cortex (S1) (22 voxels), with the second positioned more medially and closer to corticospinal tract (92 voxels). There were no significant regions of white matter in the 'ketamine > controls' contrast. The same analysis was conducted using the radial diffusivity data; however, no significant differences were found between the groups for either contrast. To explore the laterality of the effects further, we performed an additional ketamine > controls and controls > ketamine analysis restricted to either the left or the right hemisphere using a volume of interest. This analysis confirmed the finding of abnormalities present in the right hemisphere, with the

Table 1 Details of Demographic Characteristics and Drug Use of Patients with Ketamine Dependence and Control Participants

	Ketamine dependent (n = 16)		Control subjects (n = 16)	
Demographic variables				
Age, mean ± SD, years	27.00	6.74	28.5	5.74
Range, years	19–46		21–43	
Female, n (%)	7	43.75	5	31.25
Education, mean ± years	16.00	4.04	17.38	4.24
Number of cigarettes smoked ± per day	7.19	10.55	2.74	5.32
Questionnaires				
OLIFE total ± SD	23.75**	5.72	15.5	5.52
DES total ± SD	949.9**	501.1	304.7	22.5
Ketamine use variables				
Age of first use, mean ± years	19.9	6.27	NA	NA
Range, years	13–40		NA	
Duration, mean ± years	7.25	3.11	NA	NA
Range, years	2–15		NA	
Ketamine days/month, mean ± SD	26.25	6.07	NA	NA
Ketamine amount grams, mean ± SD	2.75	1.44	NA	NA
Other Drug Use	4		3	
MDMA, n regular users				
MDMA days/month, mean ± SD	1.14	2.60	0.55	1.05
MDMA per session in tablets, mean ± SD	1.0	2.27	0.87	1.35
Alcohol, regular users	9		12	
Alcohol days/month, mean ± SD	12.75	10.34	13.1	10.58
Alcohol per session in units, mean ± SD	5.34	4.94	5.62	2.28
Cannabis, n regular users	7		8	
Cannabis days/month, mean ± SD	6.88	8.95	6.0	8.53
Cannabis per session in joints, mean ± SD	1.47	2.50	0.72	1.43
Speed, n regular users	2		1	
Speed days/month, mean ± SD	1.88	4.29	0.24	0.52
Speed amount per session in grams, mean ± SD	0.34	0.89	0.13	0.29
Benzodiazepines, no. of regular users	3		1	
Benzodiazepines days/month, mean ± SD	2.31	5.41	0.23	0.78
Benzodiazepines per session amount mg, mean ± SD	4.56	10.24	0.11	0.30
Cocaine, n regular users	6		7	
Cocaine days/month, mean ± SD	3.19	4.62	0.82	1.41
Cocaine amount, mean ± SD	0.45	0.60	0.31	0.62

Abbreviation: NA, not applicable.

location of the clusters the same as the original observation but slightly increased in size, likely because of the reduced number of multiple comparisons. We also analyzed left versus right asymmetries and made a between-group comparison to look for a hemisphere by group interaction. This analysis revealed no significant effect, with the ketamine users showing no larger asymmetry in white matter compared with the controls. We also examined whether the variation across individuals in the mean D_P within each cluster was associated with total lifetime ketamine use, recency of ketamine use, or scores on the OLIFE and DES questionnaires using the bivariate correlation analysis (using an adjusted alpha level of 0.01 because of multiple comparisons). However, this did not reveal any significant correlations between the ketamine-use data or questionnaire scores, in contrast to the only other investigation of chronic ketamine use and white matter microstructure (Liao et al, 2010).

Probabilistic Tractography Analysis

We examined the connectivity profile between the caudate nucleus and three prefrontal regions in both left and right hemispheres (See Figure 1). We first explored whether the control and ketamine groups differed in terms of cortico-subcortical total percentage connectivity. In the left hemisphere, we found no significant differences between the groups in terms of the connectivity between the caudate nucleus and LPFC (independent samples t-test; $P < 0.48$) and MFC ($P < 0.31$) or OFC ($P > 0.79$). The same case was evident in the right hemisphere, with no significant difference between the groups in LPFC ($P > 0.9$), MFC ($P > 0.5$), or OFC ($P > 0.8$). We then investigated whether the CDRs demonstrated any significant difference in size between the groups. Here we found no significant differences in the right hemisphere—LPFC ($P > 0.63$), MFC ($P > 0.62$), and OFC ($P > 0.23$)—or the left hemisphere—LPFC ($P > 0.84$), MFC ($P > 0.83$), or OFC ($P > 0.79$). There was also no significant difference in volume of the cortical or subcortical ROIs between the groups in either the right or the left hemisphere (see Supplementary Table 1 and Figure 1); therefore, these findings are independent of ROI size.

We then examined whether individual differences in the connectivity profile within the ketamine group were associated with their estimated total exposure to ketamine, or their dissociative or psychosis-like symptoms indexed by DES and OLIFE scores. Pearson correlations were performed (again using an alpha level of 0.01); a Shapiro–Wilk test for normality confirmed that this was appropriate ($P > 0.19$). This revealed a highly significant positive correlation between DES score and caudate–LPFC connectivity in the right hemisphere ($r = 0.65$, $P < 0.006$) but not in the left hemisphere ($r = 0.28$, $P > 0.29$) (see Figure 3). To test for differences between the left and right LPFC-caudate correlations, we used a Fisher Z test for dependent samples. This revealed a significant difference between the correlations in each hemisphere ($t = 1.79$, $P < 0.05$, one-tailed). No significant associations were found between caudate connectivity and MFC or OFC; there were no significant correlations between connectivity and OLIFE or total ketamine use in either hemisphere.

In summary, our main findings were of decreased axial diffusivity (microstructural integrity) of white matter pathways in the right hemisphere, most prominently underlying the prefrontal cortex. Furthermore, probabilistic tractography

Table 2 Location of Significant Differences in White Matter Microstructure Between Groups as Measured by Axial Diffusivity

		Size (voxels)	T stat	Tmax			CoM		
				x	y	z	x	y	z
1	Anterior corona radiata	671	3.972	27	30	6	28	22	2
2	Forceps minor	177	3.966	18	45	− 8	20	45	5
3	SLF (near intraparietal sulcus)	173	4.71	29	− 45	36	32	− 42	35
4	Posterior thalamic radiation/IFOF	165	3.482	31	− 40	16	32	− 38	16
5	SLF (CST)	92	3.637	34	− 12	39	33	− 15	39
6	Sagittal stratum/IFL/IFOF	38	2.49	38	− 11	− 15	37	− 11	− 13
7	Anterior forceps minor	34	4.345	17	56	1	17	54	0
8	SLF/S1	22	3.256	49	− 6	23	46	− 6	24

Abbreviations: IFL, inferior longitudinal fasciculus; IFOF, Fronto-occipital fasciculus; S1, primary somatosensory cortex.
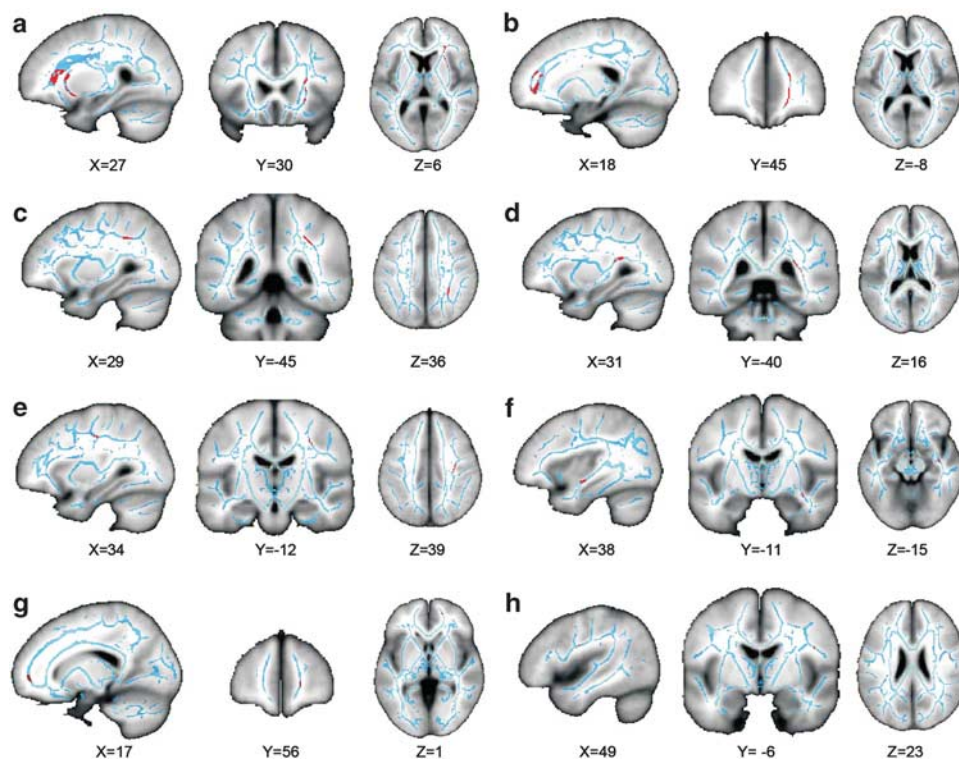
Figure 2 Location of significant differences in white matter microstructure between groups in anterior regions as measured by axial diffusivity. The location of the clusters of voxels that had significantly lower D_P diffusivity in the patient group compared with the controls. The clusters (highlighted in red) are superimposed on a structural T1 image (gray), and the skeletonized FA image (blue), coordinates given in mm. (a) Region in anterior corona radiata, (b) forceps minor, (c) SLF close to intraparietal sulcus, (d) posterior thalamic radiation/IFOF, (e) SLF close to CST, (f) Sagittal stratum/IFL/IFOF, (g) anterior forceps minor, and (h) SLF/SI.

revealed a significant positive correlation between the caudate–LPFC connectivity and a predisposition to dissociative (psychotic) symptoms in, and only in, the right hemisphere.

DISCUSSION

The aim of this investigation was to examine whether individuals who have used ketamine recreationally for a number of years exhibit differences in brain white matter structure compared with healthy volunteers. We replicated

previous findings of increased dissociative and schizotypal symptoms in ketamine users. Our control group was very similar to the ketamine group for the use of psychotropic drugs other than ketamine.

One of the main findings of the study was of widespread reductions in axial diffusivity in the ketamine group compared with the controls. Interestingly, all the clusters were lateralized to the right hemisphere. The two largest clusters were located in the prefrontal cortex: the first close to the white matter of the anterior corona radiata and the second positioned more anteriorly in part of the forceps minor. We also found evidence that dissociative symptoms
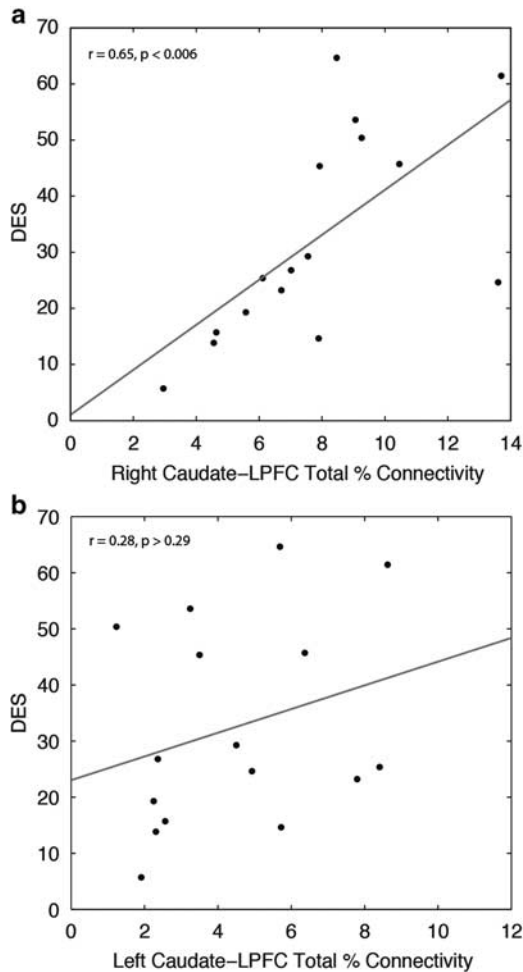
Figure 3 Correlation between DES score and caudate–LPFC connectivity in the right hemisphere. Within the ketamine-user group, there was a significant correlation between DES score and caudate–LPFC total percentage connectivity in the right hemisphere (a), normalized for each individual's caudate volume, but no significant correlation was found between DES score and caudate–LPFC connectivity in the left hemisphere (b).

in ketamine users were related to differences in connectivity between the caudate and the prefrontal cortex.

To date, there has only been one report examining white matter structure in chronic ketamine users (Liao et al, 2010). This identified three areas where FA differed in ketamine users compared with controls, located bilaterally in the frontal cortex. Our findings partially concur with those results, as the largest areas of difference that we noted between ketamine and control groups were also located in the prefrontal white matter. The origins of these prefrontal white matter differences in ketamine users are not yet clear. Ketamine acutely elevates levels of prefrontal cortical glutamate at AMPA/kainite receptors (Moghaddam et al, 1997), and it is known that forebrain white matter oligodendrocytes are vulnerable to AMPA/kainite receptor-mediated excitotoxicity (for example, Mcdonald et al (1998)). Although oligodendrocytes are highly vulnerable to glutamate-mediated excitotoxicity, there is also evidence to suggest that axons may also be susceptible through direct activation of axon-based receptors in addition to indirect effects because of the toxicity of neighboring cells (Pitt et al,

2010). Therefore, sustained excess glutamate in ketamine users as a consequence of repeated NMDA-receptor antagonism may produce these frontal abnormalities through an excitotoxic mechanism. However, white matter frontal abnormalities have been observed in a variety of drug-dependent populations (Goldstein and Volkow, 2002) and therefore this may alternatively reflect a more general consequence of, and/or vulnerability to, drug addiction.

We chose to compare both axial and radial directions of diffusivity, rather than FA, in order to make inferences about the physiological basis for the difference in diffusivity. The axial diffusion direction is thought to reflect the packing density and diameter of axons (Song et al, 2003). Therefore, the finding of distributed changes in axial diffusivity is more likely because of differences in the size, number, or arrangement of axons in the ketamine group, as opposed to differences in myelination. Although oligodendrocytes are thought to modulate a significant proportion of the radial diffusivity, this relationship does not always hold in situations where the local topology of white matter includes areas of crossing fibers or voxel size (Alexander and Seunarine, 2010; Oouchi et al, 2007). A possible explanation for observing only axial differences may be that localized glutamate excitotoxicity would affect oligodendrocytes and hence radial diffusivity in a focal region, but could potentially propagate over a much larger area while affecting axons. This could lead to more detectable differences because of axonal damage, and less sensitivity to changes in radial diffusivity. A second consideration is that the ketamine abusers in this study have used ketamine for a number of years, with some individuals beginning to use ketamine during adolescence, which is a stage of development known to involve significant brain plasticity(Blakemore and Choudhury, 2006). Therefore, although one might expect to see significant changes in radial diffusivity because of demyelination, the pattern of changes in brain white matter microstructure associated with chronic ketamine use is likely to be more complex. We also examined whether chronic, heavy ketamine use was associated with differences in subcortical–cortical brain connectivity between the caudate nucleus and the three prefrontal regions. This approach revealed no differences between the groups in terms of the proportion of connections from caudate to LPFC, MFC, or OFC. The structural variation across individuals in the ketamine group was then examined to determine whether this was related to total lifetime ketamine use or to schizotypal or dissociative symptoms, as measured by the OLIFE and DES. A significant correlation emerged between caudate–LPFC connectivity in the right hemisphere and the DES score. This finding is particularly interesting because the level of frontal activation during an associative learning task has also been shown to correlate with the DES score, when healthy controls were administered an acute dose of ketamine (Corlett et al, 2006). Therefore, paradoxically higher structural integrity in this pathway in chronic ketamine users might result in increased dissociative symptoms in everyday life. Perhaps this reflects a system that is more vulnerable to perturbation. As we found no significant difference between the groups in cortic–striatal connectivity, this finding has to be considered in the

context of the right-lateralized differences in axial diffusivity. It may be the case that the right hemisphere differences in axial diffusivity provide a 'platform' from which variability in caudate–LPFC connectivity determines the severity of dissociative experience.

None of our findings correlated with self-reported estimates of ketamine use. Recent work into brain structural differences associated with addiction has demonstrated that the siblings of addicts demonstrate similar patterns of white and gray matter brain structural alterations when compared with non-related controls (Ersche *et al*, 2012). Therefore it is possible that the right hemispheric differences observed here would not necessarily correlate with total lifetime ketamine consumption, as these differences may be related to 'cause' rather than 'effect' of drug use.

The other previous study of white matter abnormalities in ketamine users found bilateral frontal cortex differences in FA, but also differences in the left temporoparietal cortex (Liao *et al*, 2010). The differences between that study and our findings could be because of several factors. Their group sizes were greater, and this could have increased sensitivity for detecting changes in both hemispheres. However, the reduced number of diffusion-sensitizing directions used in the sequence by Liao *et al* (2010) may have balanced this effect. A further consideration is the processing and analysis of the diffusion-weighted data. For the voxelwise analysis, we chose to use tract-based spatial statistics. This approach uses the centers of white matter tracts to align white matter structure between individuals, with the aim of improving the sensitivity of white matter comparisons across participants, and it represents a more conservative approach to white matter alignment (Smith *et al*, 2006). Therefore, with our approach we might expect to achieve greater sensitivity to detect more focal differences between the groups. The further analyses we performed to interrogate the laterality of the differences suggest that, although we found only right-lateralized abnormalities when the volume of interest was restricted to a single hemisphere, the lack of a group by hemisphere interaction does not exclude the possibility that abnormalities are present in both hemispheres. Therefore, the preponderance for larger right hemisphere effects may be associated with chronic ketamine use, or the differences may represent insufficient statistical power to detect differences in both hemispheres.

Our findings are also interesting in relation to the disconnection hypothesis for schizophrenia: indeed, the subtle and regionally specific changes we have observed in chronic ketamine users are not dissimilar from the early anatomical models of psychosis (for example, metachromatic leukodystrophy) that furnished an early metaphor for schizophrenia as a disconnection syndrome (Lipska *et al*, 1995; Friston and Frith 1995). Furthermore, 'numerous studies suggested that there are functional disconnections between several cerebral integrative brain regions in schizophrenia, namely the prefrontal cortex and striatum' (Meyer and Louilot, 2012). Both dopaminergic (DA) and glutamatergic abnormalities have also been proposed in schizophrenia and non-competitive NMDA antagonists, such as ketamine, cause psychotic states in normal subjects and exacerbate symptoms in schizophrenics. Recently, it has been suggested that striatal DA dysregulation could be

the result of a prefronto–striatal disconnectivity involving glutamatergic NMDA receptors (Jentsch and Roth, 1999; Laruelle *et al*, 2005). This hypothesis has been addressed recently by using tetrodotoxin (TTX) disconnection of the left PFC in rats during the perinatal period and by assessing responses to ketamine in adulthood (Meyer and Louilot, 2012). Crucially, DA increase in the nucleus accumbens in adult animals—after administration of ketamine—was greater in TTX-microinjected (disconnected) animals than in control animals. These results suggest that prefrontal disconnections could render subjects more sensitive to ketamine-induced dopamine responses and speak to disconnection as a potential contributor to ketamine addiction.

It is notable that both our microstructural and tractography results suggest a right hemisphere lateralization for frontal disconnections. A similar, and perhaps counterintuitive, right lateralization was also the primary finding in a functional magnetic resonance imaging study of associative learning in normal subjects using ketamine: low-dose ketamine perturbed prediction error-dependent learning activity in, and only in, the right LPF—the same region implicated by our anatomical results. Crucially, subjects showing the highest degree of prefrontal activation with placebo showed the greatest perceptual aberrations and ideas or delusions of reference in response to ketamine (Corlett *et al*, 2006). As noted by the authors, 'these findings relate aberrant prediction error-dependent associative learning to referential ideas and delusions via a perturbation of frontal cortical function.' From the perspective of our findings, the associative learning in this study typically engages DA projections to the basal ganglia.

In summary, we compared brain white matter structure of chronic ketamine users with healthy controls and found widespread alterations to indices of white matter microstructure. We then investigated whether these changes would affect connectivity between brain regions thought to be modulated by ketamine use and found that individual variability within the ketamine group in the right hemisphere caudate–LPFC pathway positively correlated with dissociative-experience scores. These findings suggest that chronic ketamine use is associated with significant changes to white matter microstructure in the brain, and this may contribute to the higher frequency of dissociative experiences reported by chronic ketamine users. This has implications for our understanding of the effects of chronic ketamine administration on the brain structure and the role of anatomical connectivity in predicting the individual differences in symptomatology.

FUNDING AND DISCLOSURE

REFERENCES

Alexander DANIELC, Seunarine KIRANK (2010). Mathematics of Crossing Fibers.. *Diffusion MRI: Theory, Methods, and Applications*. Oxford University Press: New York, NY, USA, pp 451–464.

Baddeley A, Emslie H, Nimmo Smith I (1993). The spot-the-word test: a robust estimate of verbal intelligence based on lexical decision. *Br J Clin Psychol* **32**: 55–65.

Basser PJ, Mattiello J, Lebihan D (1994). Estimation of the effective self-diffusion tensor from the Nmr Spin-Echo. *J Magn Reson B* **103**: 247–254.

Beaulieu C (2002). The basis of anisotropic water diffusion in the nervous system - a technical review. *NMR Biomed* **15**: 435–455.

Behrens TEJ, Johansen-Berg H, Woolrich MW, Smith SM, Wheeler-Kingshott CAM, Boulby PA et al (2003). Non-invasive mapping of connections between human thalamus and cortex using diffusion imaging. *Nat Neurosci* **6**: 750–757.

Bernstein EM, Putnam FW (1986). Development, reliability, and validity of a dissociation scale. *J Nerv Ment Dis* **174**: 727–735.

Blakemore S-J, Choudhury S (2006). Development of the adolescent brain: implications for executive function and social cognition. *J Child Psychol Psychiatr* **47**: 296–312.

Brozoski TJ, Brown RM, Rosvold HE, Goldman PS (1979). Cognitive deficit caused by regional depletion of dopamine in prefrontal cortex of rhesus monkey. *Science* **205**: 929–932.

Corlett PR, Honey GD, Aitken MRF, Dickinson A, Shanks DR, Absalom AR et al (2006). Frontal responses during learning predict vulnerability to the psychotogenic effects of ketamine: linking cognition, brain activity, and psychosis. *Arch Gen Psychiatry* **63**: 611.

Corlett PR, Honey GD, Fletcher PC (2007). From prediction error to psychosis: ketamine as a pharmacological model of delusions. *J Psychopharmacol* **21**: 238–252.

Dawson N, Morris BJ, Pratt JA (2011). Subanaesthetic ketamine treatment alters prefrontal cortex connectivity with thalamus and ascending subcortical systems. *Schizophr Bull* **39**: 366–377.

Deichmann R, Schwarzbauer C, Turner R (2004). Optimisation of the 3D MDEFT sequence for anatomical brain imaging: technical implications at 1.5 and 3T. *Neuroimage* **21**: 757–767.

Desikan RS, Ségonne F, Fischl B, Quinn BT, Dickerson BC, Blacker D et al (2006). An automated labeling system for subdividing the human cerebral cortex on MRI scans into gyral based regions of interest. *Neuroimage* **31**: 968–980.

Eickhoff SB, Stephan KE, Mohlberg H, Grefkes C, Fink GR, Amunts K et al (2005). A new SPM toolbox for combining probabilistic cytoarchitectonic maps and functional imaging data. *Neuroimage* **25**: 1325–1335.

Ersche KD, Jones PS, Williams GB, Turton AJ, Robbins TW, Bullmore ET (2012). Abnormal brain structure implicated in stimulant drug addiction. *Science* **335**: 601–604.

Friston KJ, Frith CD (1995). Schizophrenia: a disconnection syndrome. *Clin Neurosci* **3**: 89–97.

Goldstein RZ, Volkow ND (2002). Drug addiction and its underlying neurobiological basis: neuroimaging evidence for the involvement of the frontal cortex. *Am J Psychiatry* **159**: 1642.

Honey GD, Corlett PR, Absalom AR, Lee M, Pomarol-Clotet E, Murray GK et al (2008). Individual differences in psychotic effects of ketamine are predicted by brain function measured under placebo. *J Neurosci* **28**: 6295–6303.

Jansons KM, Alexander DC (2003). Persistent angular structure: new insights from diffusion magnetic resonance imaging data. *Inf Process Med Imaging* **18**: 672–683.

Jentsch JD, Roth RH (1999). The neuropsychopharmacology of phencyclidine: from NMDA receptor hypofunction to the dopamine hypothesis of schizophrenia. *Neuropsychopharmacology* **20**: 201–225.

Krystal JH, Karper LP, Seibyl JP, Freeman GK, Delaney R, Bremner JD et al (1994). Subanesthetic effects of the noncompetitive NMDA antagonist, ketamine, in humans: psychotomimetic, perceptual, cognitive, and neuroendocrine responses. *Arch Gen Psychiatry* **51**: 199.

Laruelle M, Frankle WG, Narendran R, Kegeles LS, Adi-Dargham A (2005). Mechanism of action of antipsychotic drugs: from dopamine D(2) receptor antagonism to glutamate NMDA facilitation. *Clin Ther* **27**: S16–S24.

Liao Y, Tang J, Corlett PR, Wang X, Yang M, Chen H et al (2011). Reduced dorsal prefrontal gray matter after chronic ketamine use'. *Biol Psychiatry* **69**: 42–48.

Liao Y, Tang J, Ma M, Wu Z, Yang M, Wang X et al (2010). Frontal white matter abnormalities following chronic ketamine use: a diffusion tensor imaging study. *Brain* **133**: 2115.

Lipska BK, Weinberger DR, Swerdlow NR, Geyer MA, Braff DL, Jaskiw GE (1995). Neonatal excitotoxic hippocampal damage in rats causes post-pubertal changes in prepulse inhibition of startle and its disruption by apomorphine. *Psychopharmacology* **122**: 35–43.

Marenco S, Stein JL, Savostyanova AA, Sambataro F, Tan HY, Goldman AL et al (2011). Investigation of anatomical thalamo-cortical connectivity and fmri activation in schizophrenia. *Neuropsychopharmacology* **37**: 499–507.

Mason O, Claridge G, Jackson M (1995). New scales for the assessment of schizotypy. *Pers Individ Dif* **18**: 7–13.

Mcdonald JW, Althomsons SP, Hyrc KL, Choi DW, Goldberg MP (1998). Oligodendrocytes from forebrain are highly vulnerable to AMPA/kainate receptor-mediated excitotoxicity. *Nat Med* **4**: 291–297.

Meyer F, Louilot A (2012). Early prefrontal functional blockade in rats results in schizophrenia-related anomalies in behavior and dopamine. *Neuropsychopharmacology* **37**: 2233–2243.

Moghaddam B, Adams B, Verma A, Daly D (1997). Activation of glutamatergic neurotransmission by ketamine: a novel step in the pathway from NMDA receptor blockade to dopaminergic and cognitive disruptions associated with the prefrontal cortex. *J Neurosci* **17**: 2921–2927.

Morgan CJA, Monaghan L, Curran HV (2004a). Beyond the K-hole: a 3-year longitudinal investigation of the cognitive and subjective effects of ketamine in recreational users who have substantially reduced their use of the drug. *Addiction* **99**: 1450–1461.

Morgan CJA, Mofeez A, Brandner B, Bromley L, Curran HV (2004b). Acute effects of ketamine on memory systems and psychotic symptoms in healthy volunteers. *Neuropsychopharmacology* **29**: 208–218.

Morgan CJA, Muetzelfeldt L, Curran HV (2010). Consequences of chronic ketamine self-administration upon neurocognitive function and psychological wellbeing: a 1-year longitudinal study. *Addiction* **105**: 121–133.

Mori S, Wakana S, Van Zijl PCM, Nagae-Poetscher LM (2005). *MRI Atlas of Human White Matter*. Elsevier: Amsterdam, The Netherlands.

Narendran R, Frankle WG, Keefe R, Gil R, Martinez D, Slifstein M et al (2005). Altered prefrontal dopaminergic function in chronic recreational ketamine users. *Am J Psychiatry* **162**: 2352–2359.

Nichols T. E, Holmes A. P (2002). Nonparametric permutation tests for functional neuroimaging: a primer with examples. *Hum Brain Mapp* **15**: 1–25.

Oouchi H, Yamada K, Sakai K, Kizu O, Kubota T, Ito H et al (2007). Diffusion anisotropy measurement of brain white matter is affected by voxel size: underestimation occurs in areas with crossing fibers. *Am J Neuroradiol* **28**: 1102–1106.

Pitt David, Gonzales E, Cross AH, Goldberg MP (2010). Dysmyelinated axons in shiverer mice are highly vulnerable to A-amino-3-hydroxy-5-methylisoxazole-4-propionic acid (AMPA) receptor-mediated toxicity. *Brain Res* **1309**: 146–154.

Reese TG, Heid O, Weisskoff RM, Wedeen VJ (2003). Reduction of Eddy-current-induced distortion in diffusion MRI using a twice-refocused spin echo. *Magn Reson Med* **49**: 177–182.

Smith SM, Jenkinson M, Johansen-Berg H, Rueckert D, Nichols TE, Mackay CE et al (2006). Tract-based spatial statistics: voxelwise analysis of multi-subject diffusion data. *Neuroimage* **31**: 1487–1505.

Smith S. M (2002). Fast robust automated brain extraction. *Hum Brain Mapp* **17**: 143–155.

Smith SM, Jenkinson M, Woolrich MW, Beckmann CF, Behrens TEJ, Johansen-Berg H et al (2004). Advances in functional and structural MR image analysis and implementation as FSL. Neuroimage 23: 208–219.

Song SK, Sun SW, Ju WK, Lin SJ, Cross AH, Neufeld A. H (2003). Diffusion tensor imaging detects and differentiates axon and myelin degeneration in mouse optic nerve after retinal ischemia. Neuroimage 20: 1714–1722.

Song SK, Yoshino J, Le TQ, Lin SJ, Sun SW, Cross AH et al (2005). Demyelination increases radial diffusivity in corpus callosum of mouse brain. Neuroimage 26: 132–140.

Verma A, Moghaddam B (1996). NMDA receptor antagonists impair prefrontal cortex function as accessed via spatial delayed alternation performance in rats: modulation by dopamine. J Neurosci 16: 373–379.

Wakana S, Caprihan A, Panzenboeck MM, Fallon JH, Perry M, Gollub RL et al (2007). Reproducibility of quantitative tractography methods applied to cerebral white matter. Neuroimage 36: 630–644.

Wheeler-Kingshott CAM, Hickman SJ, Parker GJM, Ciccarelli O, Symms MR, Miller DH et al (2002). Investigating cervical spinal cord structure using axial diffusion tensor imaging. Neuroimage 16: 93–102.

Supplementary Information accompanies the paper on the Neuropsychopharmacology website (http://www.nature.com/npp)